Age-Related Macular Degeneration and Retinal Protein Modification by 4-Hydroxy-2-nonenal

Cheryl M. Ethen,[1] *Cavan Reilly,*[2] *Xiao Feng,*[3] *Timothy W. Olsen,*[3] *and Deborah A. Ferrington*[3]

PURPOSE. Oxidative damage to proteins, lipids, and DNA has been suggested to be a mechanism for age-related macular degeneration (AMD). The retina is particularly susceptible to lipid peroxidation due to high concentrations of easily oxidized polyunsaturated fatty acids in the presence of abundant oxygen. One of the most toxic products of lipid peroxidation, 4-hydroxy-2-nonenal (HNE), can modify and inactivate proteins. The hypothesis was that 4-HNE-modified proteins would accumulate and serve as a marker for progressive stages of AMD.

METHODS. Proteins containing HNE adducts were identified in both the macular and peripheral regions during four progressive stages of AMD. The proteins were resolved by two-dimensional (2-D) gel electrophoresis before detection of HNE-adducted proteins. Modified proteins were identified by matrix-assisted laser desorption ionization time-of-flight mass spectrometry (MALDI-TOF/MS). The total content of HNE adducts was compared using a slot blot immunoassay. One-dimensional Western blot analysis was used to measure levels of proteins involved in HNE detoxification.

RESULTS. Nineteen proteins that were consistently modified regardless of stage of AMD or retinal region were identified. These proteins are involved in two main functions: energy production and stress response. No change in total HNE-adducted protein was observed between regions or stages. Modest increases in content of proteins involved in HNE detoxification were observed.

CONCLUSIONS. Consistently modified proteins indicate preferred protein targets for oxidation by HNE. HNE-modified proteins were not different between regions or stages, suggesting that pathways for detoxification of HNE or removal of damaged proteins are adequate. Consistent levels of HNE-modified proteins suggest that HNE is not a sensitive retinal biomarker for AMD. (*Invest Ophthalmol Vis Sci.* 2007;48:3469–3479) DOI: 10.1167/iovs.06-1058

Age-related macular degeneration (AMD) is the leading cause of vision loss and blindness in individuals over the age of 65 in the developed world[1–3] and is characterized by the loss of central vision. The currently accepted, clinical grading system has been described in the Age-Related Eye Disease Study (AREDS).[4] We have described the Minnesota Grading System (MGS) for eye bank eyes, based on specific definitions used in the AREDS classification.[5] Use of the MGS provides a unique opportunity to track molecular changes in the proteome over the course of the disease, from onset to loss of central vision.[6–8]

Oxidative stress has been proposed as a possible cause of the progression of AMD.[9–16] The retina is particularly susceptible to oxidative stress because of its high metabolic activity, oxygen tension, and concentration of easily oxidized polyunsaturated fatty acids (PUFAs), as well as the presence of retinal pigments that generate reactive oxygen species when illuminated by light.[17] Protein adducts, such as advanced glycation end-products, malondialdehyde, and carboxyethylpyrrole, are indicators of oxidative stress that have been observed to increase in plasma[18,19] and the retina[19–21] with AMD. Considering the high concentration of PUFAs and the susceptibility of the retina to lipid peroxidation,[17] we sought to test the hypothesis that AMD is also associated with increased accumulation of 4-hydroxynonenal (HNE), the most cytotoxic aldehyde formed during lipid peroxidation.[22] HNE can covalently modify histidine, cysteine, and lysine residues of proteins, leading to stable HNE-protein adducts. The addition of HNE adducts to both membrane and soluble proteins has been shown to cause functional impairment.[23–26] The high level of HNE-modified retinal proteins reported in previous studies suggests that HNE is abundant in the retina.[27,28] Most important, several different models involving retinal damage have reported an increase in HNE-modified proteins.[27–29] The goal of this study is to test whether HNE is a good retinal biomarker for AMD.

In the present study, we performed separate analyses of the macular and peripheral retina at four distinct stages of AMD. The macular and peripheral retina may exhibit differences in susceptibility to HNE-induced damage due to the increased susceptibility of the aged macula to lipid peroxidation[30] and differences in antioxidant enzymatic activity[31] and fatty acid composition.[32] Using high-resolution two-dimensional (2-D) gel electrophoresis, Western immunoblot, and mass spectrometry (MS), we identified HNE-modified retinal proteins and found that most proteins are consistently present in both retinal regions at all stages of AMD. Because no accumulation of modified proteins was observed, we conclude that pathways that detoxify HNE or remove damaged proteins are sufficient to maintain steady state levels of HNE-modified proteins. The consistent level of HNE-modified proteins indicates that HNE is not a sensitive retinal biomarker for AMD.

From the Departments of [1]Biochemistry, Molecular Biology, and Biophysics and [3]Ophthalmology, and the [2]Division of Biostatistics, University of Minnesota, Minneapolis, Minnesota.

Supported in part by Grant EY014176 from the National Eye Institute (DAF) and Grant AG025392 from the National Institute on Aging (TWO); a Career Development Award from the American Federation for Aging Research; and funding from the Foundation Fighting Blindness (DAF), the American Health Assistance Foundation, the Minnesota Medical Foundation, the University of Minnesota Academic Health Center and Graduate School, and the Fesler-Lampert Foundation; and an unrestricted grant to the Department of Ophthalmology from Research to Prevent Blindness. CME was supported with Training Grant for Vision Science T32-EY07133 from the National Eye Institute.

Submitted for publication September 6, 2006; revised November 16, 2006, and March 2, 2007; accepted May 17, 2007.

Disclosure: **C.M. Ethen**, None; **C. Reilly**, None; **X. Feng**, None; **T.W. Olsen**, None; **D.A. Ferrington**, None

The publication costs of this article were defrayed in part by page charge payment. This article must therefore be marked "*advertisement*" in accordance with 18 U.S.C. §1734 solely to indicate this fact.

Corresponding author: Deborah A. Ferrington, 380 Lions Research Building, 2001 6th Street SE, Minneapolis, MN 55455; ferri013@umn.edu.

METHODS

Grading Donor Eyes for the Level of AMD

The donor eyes used in this study were obtained from the Minnesota Lions Eye Bank. Written consent was acquired from the donor or donor family for use in medical research in accordance with the principals outlined in the Declaration of Helsinki. Dissection of the sensory retina was performed as reported previously.[8] Criteria established by the MGS were used to determine the stage of AMD.[5] The stages of AMD are referred to as MGS1 (minimal or no AMD) through MGS4 (severe AMD) and correspond directly with the AREDS classification system.[4] MGS1 represents our control group and includes donors with either no or a few small drusen. MGS2 is considered early-stage AMD (more numerous small drusen and possible pigmentary changes). MGS3 is defined by at least 20 intermediate-sized drusen, a single large druse, or noncentral subfoveal geographic atrophy. Advanced AMD (MGS4) corresponds to central macular damage from either geographic atrophy or active choroidal neovascularization. Based on donor information records and clinical examination of the neurosensory tissue, donor eyes were screened for and excluded if other ocular diseases were observed, such as glaucoma or diabetic retinopathy.

Preparation of Retinal Homogenates

Retinal homogenates were prepared as described.[8] In brief, a trephine punch of 8-mm diameter was centered over the macular area to separate the macula from the periphery. The neurosensory retina was carefully dissected from the RPE and homogenized in a buffer containing 20% sucrose, 20 mM Tris-acetate (pH 7.2), 2 mM $MgCl_2$, 10 mM glucose, and 2% CHAPS (3 [3-chloamidopropyl]dimethylammonio-2-hydroxy-1-propanesulfonate). The superior and nasal regions were used for peripheral studies. The homogenates were stored at −80°C. Protein concentrations were determined by the bicinchoninic acid (BCA) protein assay (Pierce Biotechnology, Rockford, IL). Bovine serum albumin (BSA) was used as a standard.

Postmortem HNE Modification

Five-month-old Fischer 344 rats were purchased from the Veterinary Medical Unit at the Minneapolis Veterans Affairs Medical Center's aging rodent colony, which is maintained by the University of Minnesota. An animal protocol was approved by the Institutional Animal Care and Use Committee of the University of Minnesota and followed guidelines established in the ARVO Statement for the Use of Animals in Ophthalmic and Vision Research. In these experiments, the conditions of human donor eyes were replicated to mimic eye bank conditions. For example, bodies were maintained at room temperature for 2.5 hours and then refrigerated until enucleation at 4.5 hours postmortem. One eye from each rat was immediately enucleated, and the retinas were dissected and frozen at −80°C. Eyes processed immediately after death served as control specimens for the remaining eyes that were dissected at one of nine time points ranging from 2 to 24 hours postmortem. Rat retinas were processed as described for human retinas. Retinal proteins were resolved by one-dimensional (1-D) SDS-PAGE, transferred, and probed with an antibody that recognizes HNE Michael adducts (1:1000; Alpha Diagnostics, San Antonio, TX). Total immune reaction per lane was quantitated (Sigma Scan; SPSS, Chicago, IL), and control reactions at time 0 were compared with reactions in companion retinas harvested at later times postmortem. Density of HNE-modified proteins at time 2 to 24 hours relative to their control were plotted versus postmortem time. Linear regression was used to test the relationship between HNE content and postmortem time.

Preparation of HNE-Modified BSA Standard

The HNE-modified BSA standard was generated by incubating BSA (Sigma-Aldrich, St. Louis, MO) with HNE (Cayman Chemical, Ann Arbor, MI).[28] Protein concentration was determined using BCA protein reagents. HNE modification of BSA was confirmed by Western immunoblot using an antibody that recognizes HNE Michael adducts (1:1000; Alpha Diagnostics).

Slot Blot Immunoassay

Relative content of HNE in human retinal homogenates was determined as previously reported in rat retina.[28] Human neurosensory retinal proteins and HNE-BSA standard were adsorbed to polyvinylidene difluoride (PVDF) membranes by using a slot blot apparatus. The antibody for HNE-adducts was used in conjunction with goat anti-rabbit alkaline phosphatase-conjugated secondary antibody (Bio-Rad, Hercules, CA) and the substrate 5-bromo-4-chlor-3′-iodolyl phosphate *p*-toluidine/nitro blue tetrazolium chloride (BCIP-NBT) to visualize the immunoreaction. The immunoreactions of the protein standard and retinal homogenates were quantified by densitometric analysis of scanned blots (Quantity One software; Bio-Rad). The relative amount of HNE in each sample was determined from the relative change in intensity as a function of protein load and compared with the HNE-BSA standard on the same PVDF membrane. The relative content of HNE in each donor sample was determined from the average of two to four separate measurements. Homogenates from six separate donors were evaluated for each stage of AMD in both the macular and peripheral regions.

Western Immunoblot of 1-D Gels

Retinal proteins were electrophoretically separated by sodium dodecyl sulfate polyacrylamide gel electrophoresis (SDS-PAGE), as previously reported.[8] After resolution of proteins by 13% SDS-PAGE, retinal proteins were electrophoretically transferred to PVDF membranes. PVDF membranes were probed with one of the primary antibodies listed in Table 1. Goat anti-mouse, goat anti-rabbit, or bovine anti-goat alkaline phosphatase-conjugated secondary antibody (1:3000) was used in conjunction with the substrate BCIP-NBT to visualize the immunoreaction. Preliminary experiments showed that retinal protein loads between 1 and 20 μg produced a linear signal when using the antibodies that detect proteins involved in detoxification pathways. Therefore, 15 μg was chosen as the amount of total protein to load for the semiquantitative Western blot analysis. Images were captured with a densitometer (model GS800; Bio-Rad).

Densitometry of Immune Reaction

To determine the relative content of proteins, densitometric analysis was performed on the immunoreaction of individual protein bands (Quantity One; Bio-Rad). All band densities were normalized to a reference sample from a peripheral retinal homogenate that was included on each Western blot. This allowed for blot-to-blot comparisons.

2-D Gel Electrophoresis

First dimension isoelectric focusing (IEF) was performed with an IEF cell (Protean IEF Cell; Bio-Rad) with 11-cm, pH 5 to 8 immobilized pH gradient (IPG) strips. IPG strips were rehydrated and focused with 150 μg human retinal protein, as previously reported.[6] 2-D SDS-PAGE was performed after equilibration of IPG strips with dithiothreitol (DTT) and iodoacetamide, as previously reported,[6] according to Laemmli.[33] For each sample, two gels were run in parallel. One gel of each pair was silver-stained using mass spectrometry–compatible solutions (Bio-Rad). The alternate gel was used for Western immunoblot analysis. Images were then captured (Fluor-S Multi-Imaging system or GS800 densitometer; Bio-Rad).

Western Immunoblot Analysis of 2-D Western Blots

After resolution of proteins by 12% SDS-PAGE, retinal proteins were electrophoretically transferred to PVDF membrane. PVDF membranes were probed with one of the primary antibodies listed in Table 1. Due to the low signal-to-noise ratio of the HNE antibody, the signal was

TABLE 1. Antibody Information

Primary Antibody	Type	Dilution	Analysis	Company
HSP60	M	1:2500	2-D	BD Biosciences, San Jose, CA
HOP	M	1 μg/mL	2-D	StressGen, Victoria, BC Canada
CRABP	M	1:1000	2-D	Sigma-Aldrich, St. Louis, MO
DJ-1	M	1:1000	2-D	Covance, Berkley, CA
MtHSP75	M	1:2000	2-D	StressGen, Victoria, BC Canada
β-Actin	M	1:1000	2-D	Santa Cruz, Santa Cruz, CA
HSP 70	P	1:5000	2-D	StressGen, Victoria, BC Canada
Enolase	P	1:200	2-D	BioDesign, Saco, ME
GUK1	P	1:3000	2-D	Abnova, Taipei City, Taiwan
HNE	P	1:1000	2-D, SB	Alpha Diagnostics, San Antonio, TX
GCS	P	5 μg/mL	1-D	Lab Vision, Fremont, CA
ALDH	P	1:500	1-D	MorphoSys, Kingston, NH
AR	P	1:200	1-D	Santa Cruz, Santa Cruz, CA
GSTpi	P	1:1000	1-D	Calbiochem, San Diego, CA

M, monoclonal; P, polyclonal; 2-D, two-dimensional Western blot; 1-D, one-dimensional Western blot; SB, slot blot quantitation.

amplified using a streptavidin-biotin amplification system. Goat anti-rabbit biotin-conjugated secondary antibody (1:3000) was used in conjunction with streptavidin (1:3000) and biotinylated alkaline phosphatase (1:3000) and the substrate BCIP-NBT to visualize the immunoreaction. A secondary-antibody-only blot was used to eliminate false-positives and detected nonspecific immune reactions using the streptavidin amplification system (data not shown, examples of nonspecific reactions in Figs. 1, 2), and images were captured (Fluor-S MultiImaging System or GS800 Densitometer; Bio-Rad).

Immunoprecipitation

Immunoprecipitation of β-actin from retinal homogenate was performed according to the manufacturer's instructions. In brief, 300 μg of retinal homogenate was incubated with ~3 μg of β-actin antibody (Table 1) overnight at 4°C to form the antigen-antibody complex. Immobilized protein A/G resin (Pierce Biotechnology) was added and incubated an additional 2 hours before elution of the complex.

Mass Spectrometry Protein Identification

Western immunoblot analysis of 2-D gels was used to identify protein spots containing HNE adducts on proteins. To align the spots exhibiting an immunoreaction with the spots on silver-stained gels, images of Western immunoblots and their corresponding gels were printed on transparencies and overlaid on a light box, as well as aligned on computer (PDQuest 7.1.1 2D gel analysis software; Bio-Rad). Preparation of protein spots for mass spectrometry was as described.[28] Matrix-assisted laser desorption ionization-time of flight/mass spectrometry (MALDI-TOF/MS) was performed to obtain peptide mass fingerprints on either a mass spectrometer (Brüker Biflex III MALDI-TOF; Brüker Daltonics, Billerica, MA) or a quadrupole TOF mass spectrometer (QStar Pulsar; Applied Biosystems Inc., [ABI]Foster City, CA).[28] Peptide peaks were submitted to Mascot (www.matrixscience.com/ Matrix Science, Inc., Boston, MA) and compared to the NCBInr human database to obtain initial protein identification. Positive identification was based on a significant Molecular Weight Search (MOWSE) score. All searches were performed with a mass tolerance between 50 and 100 (QStar; ABI) and 100 to 225 (Biflex; Brüker Daltonics) parts per million.

Confirmation of initial identities was obtained by peptide mass sequencing using either MALDI or electrospray ionization (ESI) MS. Peptides analyzed by ESI were separated by liquid chromatography online (QStar Pulsar quadrupole TOF; ABI or LCQ Classic ion trap mass spectrometer; ThermoFinnigan, San Jose, CA) and ionized as described.[28]

Statistical Analysis

Immunoreactive proteins from 2-D analyses were analyzed by Fisher exact test (NCSS software and R statistical computing software avail-

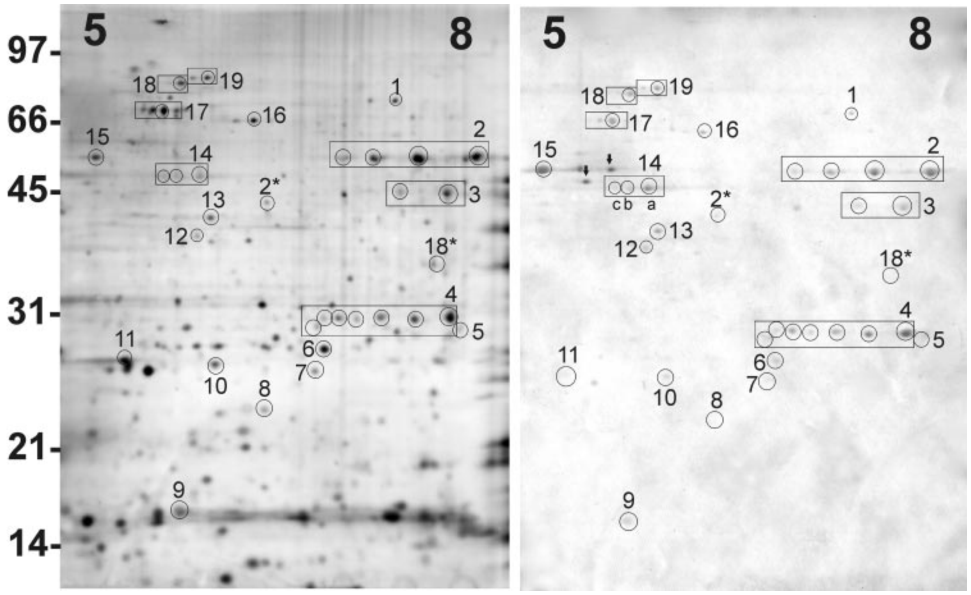

FIGURE 1. Detection of HNE-modified retinal proteins. *Left*: representative 2-D silver-stained gel (150 μg); *right*: corresponding 2-D Western blot probing for HNE-adducts. *Circled* proteins indicate immunopositive spots identified by mass spectrometry. Numbers correspond to protein identities listed in Table 3. *Boxed regions*: proteins with the same identification migrating at different isoelectric points (pI) that were identified by either MS or 2-D immunoblot analysis (Table 3). Isoelectric variants indicated as 14a, -b, and -c also correspond to Table 3. A linear pI range from 5 to 8 is indicated at the *top*. Molecular weight markers are indicated to the *left*. *Arrows*: false positive-reactions (*right*). Unlabeled immune reactions represent protein spots that were not identified due to individual donor variation. *Proteins resolved at a position inconsistent with the theoretical migration.

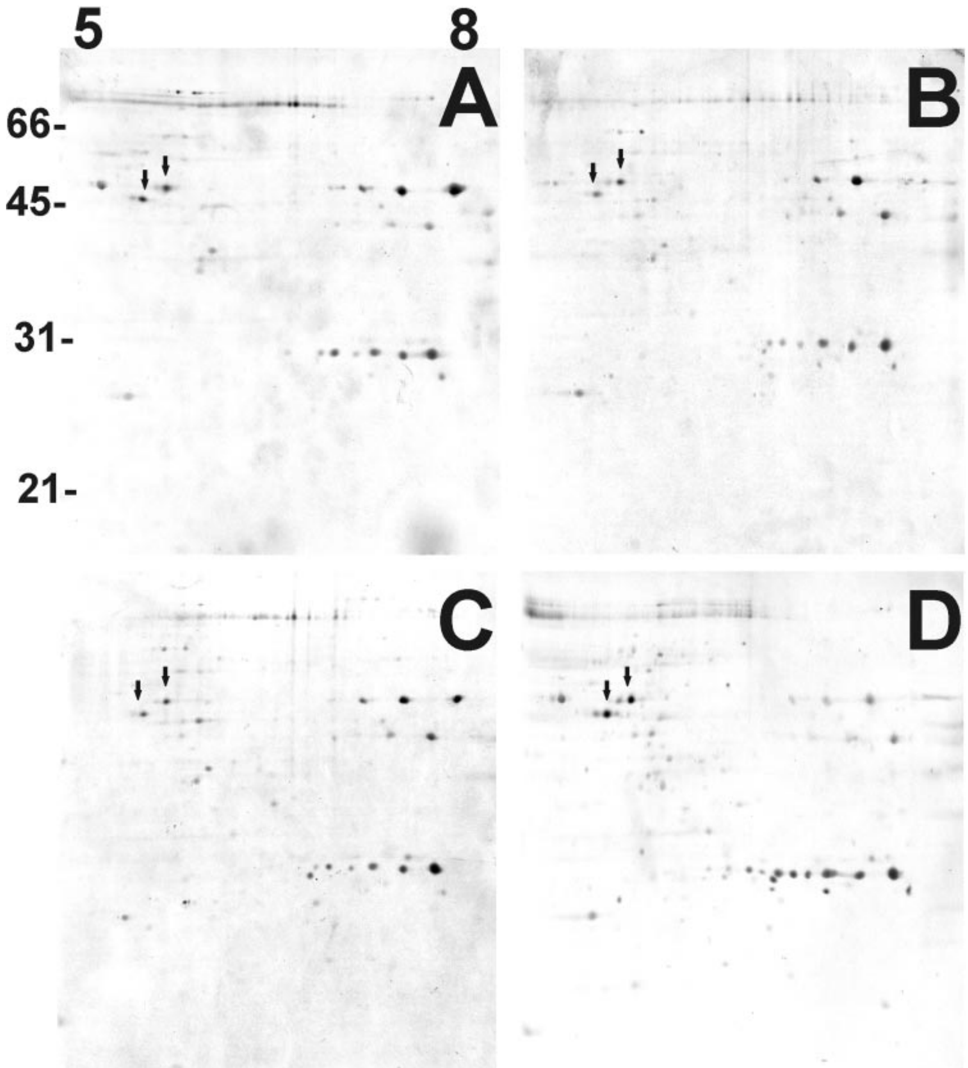

Figure 2. Western blot analysis of HNE-protein adducts. Retinal proteins (150 μg) from the macula were resolved by 2-D gel electrophoresis, transferred to PVDF membrane, and probed for HNE adducts. Shown are representative immunoblots from the macula of donors: MGS1 (**A**), MGS2 (**B**), MGS3 (**C**), MGS4 (**D**). Seven blots were analyzed for each MGS stage in the macula. Similar results were detected using retinal proteins from the peripheral region (n = 8 at each stage). *Arrows*: false-positive reactions as shown in Figure 1.

able online at www.r-project.org). We tested for changes in protein modification between stages and regions. To test for increases in frequency of modification in the macular region at each stage of the disease and for a comparison of macular and peripheral regions regardless of stage, we used a one-tailed *t*-test. Total HNE immune reaction, detected by slot blot, in either region was tested with a one-way analysis of variance (ANOVA). To compare total immune reactions from regions (macula and periphery), regardless of stage, and to test for differences between MGS1 and MGS2 to -4, the Student's *t*-test was used. If the data contained a non-normal distribution, the Whitney-Wilcoxon test was used. For 1-D Western blot analysis, linear regression analysis was used to determine whether there was a significant linear relationship between protein content and the level of AMD. Linear regression was also used to test for a relationship between HNE-modified proteins and postmortem time in donor tissue and with rat retina. All statistical tests were two sided with $\alpha = 0.05$, except as otherwise noted.

Results

Experimental Design

Donor eyes were classified into four progressive stages of AMD (MGS1 to -4).[5] MGS1 served as the control group. MGS2 represented early-stage AMD, MGS3 was the intermediate stage, and MGS4, accompanied by severe central vision loss, was considered end-stage AMD. Using donor tissue from four stages of AMD allowed us to distinguish whether HNE toxicity could contribute to the pathogenesis and progression of the disease by determining whether there is a correlation between MGS stage and accumulation of HNE-protein adducts.

Demographic and clinical information for donors obtained from written records provided by the Minnesota Lions Eye Bank is summarized in Table 2. Exclusion criteria included a history of diabetes or retinal disease other than AMD. Only eyes from white donors were used in the study.[34] Postmortem conditions before tissue preparation did not differ between the four MGS groups, including the time from death to tissue freezing (average $\pm$ SD = 17.4 $\pm$ 4.6) and were similar to conditions previously published.[6,7] Because of the broad range in tissue-freezing times among donors in our study (range, 6.0–25.5 hours), we tested levels of Michael adduct HNE-modified proteins in rats that replicated the average handling conditions for donor eyes (see the Methods section). We found no linear relationship between the quantity of HNE adducts and postmortem time in rat retina (data not shown; $P = 0.2$). One additional analysis was performed to test whether HNE adducts increased with time after death to tissue processing in donor tissue used in the present study. Linear regression analysis of HNE content showed no significant postmortem time-dependent relationship for protein adducts in the macula (P =

TABLE 2. Donor Demographic and Distribution

MGS Grade	Donor Distribution			Age (y)		TAD† (h ± SD)	Enu‡ (h ± SD)	Cause of Death (*n*)
	Male	Female	Total*	Mean ± SD	Range			
1	9	2	11	57 ± 12	37–72	17 ± 4	4.9 ± 1.0	Cancer (4), respiratory failure (2), hemorrhage (1), pneumonia (1), stroke (1), pulmonary fibrosis (1), head trauma (1)
2	9	5	14	69 ± 5	60–75	16 ± 6	4.5 ± 1.5	Cancer (8), respiratory failure (3), stroke (1), sepsis (1), necrotic bowel (1)
3	9	3	12	72 ± 7	63–86	18 ± 3	4.6 ± 1.7	Cancer (4), respiratory failure (2), heart failure (1), hemorrhage (1), stroke (1), sepsis (1), renal failure (1), age (1)
4	8	3	11	81 ± 8	70–94	17 ± 7	5.3 ± 2.8	Heart failure (3), stroke (3), respiratory failure (2), hemorrhage (1), pneumonia (1), age (1)

* Donors used for 2-D Western blots, slot blot immunoassay, and 1-D Western blots.
† TAD, time after death.
‡ Enu, time to enucleation.

0.67) or periphery ($P = 0.96$). These results indicated that postmortem time does not significantly influence the amount of HNE-modified proteins in retinal donor tissue.

The goal of this study was to determine the extent of protein oxidative damage in donor eyes at different stages of AMD. Two hypotheses were investigated. First, using HNE-protein adducts as a measure of protein oxidation, we predicted that protein oxidation would increase through progressive stages of AMD. Second, we hypothesized that the macular region experiences greater oxidative stress and hence, we would observe more extensive protein oxidation in the macula than in the periphery. Finally, we measured the content of several proteins involved in detoxifying or eliminating HNE as an indirect indicator of HNE cellular content. Because these proteins are reportedly upregulated with oxidative stress,[35–38] we predicted that their content would increase with progression of the disease.

Comparison of HNE-Modified Proteins

To determine the distribution and frequency of immune reactive proteins, retinal proteins from the same donor were resolved on two 2-D gels run in parallel. One gel was stained with silver and used for MS identification of modified proteins. The paired gel was transferred and probed with an antibody that recognizes protein HNE Michael adducts (Fig. 1). Although the specificity of this antibody has been thoroughly characterized,[39] we also compared our antibody reaction with a second antibody that recognizes the reduced carbonyl of HNE Michael adducts after chemical reduction of proteins with sodium borohydride.[24] We found good agreement between reactions with the two antibodies, thus providing additional validation for the presence of HNE adducts in specific protein spots (data not shown).

Figure 2 shows a representative immune reaction from donor tissue at each stage of AMD from the macular region. As illustrated in Figure 2, the immune reactions exhibited the same relative pattern, with only minor variations in pattern and intensity observed between individual donors. Comparison of immune reactions from seven (macula) or eight (periphery) different donors at each stage showed no significant stage-dependent ($P = 0.22$–1.00) or region-dependent ($P = 0.17$–1.00) difference in frequency of modification for immunoreactive spots (Table 3). There was one exception, spot 1, that was significantly increased in the macula ($P = 0.02$), when compared with the peripheral region at MGS3 (Table 3).

Identification of In Vivo Targets of HNE

The high reproducibility of modification for individual proteins (Table 3), suggests that HNE consistently targets specific molecules. To identify HNE-modified proteins, MS analysis of protein spots exhibiting a positive immune reaction was performed. Peptides from in-gel digests were analyzed by MALDI-TOF/MS to generate a peptide mass fingerprint that was matched to the human database to obtain an initial protein identity. Unambiguous confirmation of the protein identity was obtained by MS/MS (electrospray ionization or MALDI) peptide sequencing (Table 3, Fig. 1). Several protein identifications were further validated by a positive immune reaction with protein-specific antibodies (data not shown), as indicated in Table 3.

Proteins containing HNE adducts represent two main functional categories including energy metabolism (aldolase C, α-enolase, triose phosphate isomerase [TPI], and pyruvate dehydrogenase) and chaperone function (HSP60, HSP75, and HSP70). Three energy metabolism proteins (α-enolase, aldolase C, and TPI) were modified in all donor tissues, regardless of disease stage or region of the retina (Fig. 1, Table 3). Proteins involved in chaperone function were less consistently modified; the modification was present in ~38% to 95% of all blots (Table 3).

Nine of 20 proteins identified in the present study migrated in multiple immune-positive spots at the same apparent molecular mass, but at different isoelectric points (pI) (Fig. 1). These isoelectric variants result from posttranslational modifications that alter the intrinsic charge of the protein. Examples of charge-altering modifications include phosphorylation, deamidation, glutathionylation, and HNE modification of the side chain of lysine.[40–42] No region- or stage-specific difference in HNE-modified isoelectric variants was detected.

Although 2-D gel electrophoresis provides superior resolution of individual proteins into distinct spots, it is possible to have multiple proteins comigrating in a single spot. In this study, the presence of multiple proteins in a single spot introduced ambiguity into the identification of the protein containing the HNE adducts. This occurred for spots labeled 14 (Fig. 1), where a positive identification was obtained by mass spectrometry for creatine kinase (CK), in spots 14a, -b, and -c, and β-actin, only in spots 14b and -c. Using an antibody to β-actin, we detected β-actin localized only to spots 14b and -c (Fig. 3A), thus verifying the mass spectrometry findings. Since HNE-positive spots 14b and -c contained a mixture of both β-actin and CK, the modified protein remains ambiguous. However, because spot 14a contained only CK, we concluded that retinal

Table 3. MALDI-TOF and MS/MS Identification of HNE-Immunopositive Proteins

Spot ID	Protein	Accession No. (gi)	No. Immune Spots	MW* (kDa)	pI*	MALDI-TOF MS No. Peptides	MALDI-TOF MS % Coverage	No. MS/MS Peptides	Immune rxn (2D WB)	Frequency %†	Frequency P‡
1	HSP70/HSP90 organizing protein	5803181	2	62.6	6.4	25	46	3	X	55	0.02
2	α-Enolase	4503571	4	47.1	7.0	18	50	5	X	100	1.00
3	Aldolase C	312137	2	39.4	6.4	6	25	2		100	1.00
4	Triose phosphate isomerase	136066	6	26.9	6.5	15	73	7		100	1.00
5	Protein L-isoaspartate o-methyltransferase	4885539	1	24.6	6.7	7	37	2		85	0.92
6	RNA-binding protein regulatory subunit/DJ-1	31543380	1	19.9	6.3	9	46	5	X	75	0.22
7	Guanylate kinase	55959192	1	23.7	6.9	5	25	2	X	65	0.34
8	Nucleoside diphosphate kinase-1 isoform B	17512044	1	19.6	5.4	8	53	3		43	0.33
9	Cellular retinoic acid-binding protein	4758052	1	15.7	5.3	10	69	2	X	68	0.18
10	Thiol-specific antioxidant	32189392	1	18.5	5.2	6	43	2		65	0.38
11	Glyoxalase	5729842	1	20.8	5.1	8	26	2		87	0.18
12	Pyruvate dehydrogenase	189754	1	39.6	6.2	7	27			92	0.53
13	Dimethylarginine dimethylaminohydrolase 1	6912328	1	31.4	5.5	10	39	2		93	0.58
14 abc	Brain creatine kinase	14603055	3	42.5	5.3	12	36	3	X	90	0.43
14 bc	β Actin	14250401	2	41.3	5.6	10	38	1	X	78	0.92
15	γ-Enolase	5803011	1	47.1	5.0	4	12	2	X	98	1.00
16	Protein disulfide isomerase	6912328	1	58.0	6.0	12	22	2		83	0.77
17	HSP60	306890	2	61.2	5.7	13	28	2	X	95	0.53
18	HSP70	5729877	2	71.1	5.4	21	43	1	X	48	0.36
18*	HSP70 kDa protein 9B precursor	24234688	1	73.7	6.07	17	20			38	0.20
19	HSP75	292059	2	73.7	6.0	17	28	5	X	53	0.59

* Theoretical values.
† 60 total blots, including all stages and both regions.
‡ *P*, lowest probability obtained from the Fisher exact test comparing stages, regions, or regions at different stages.

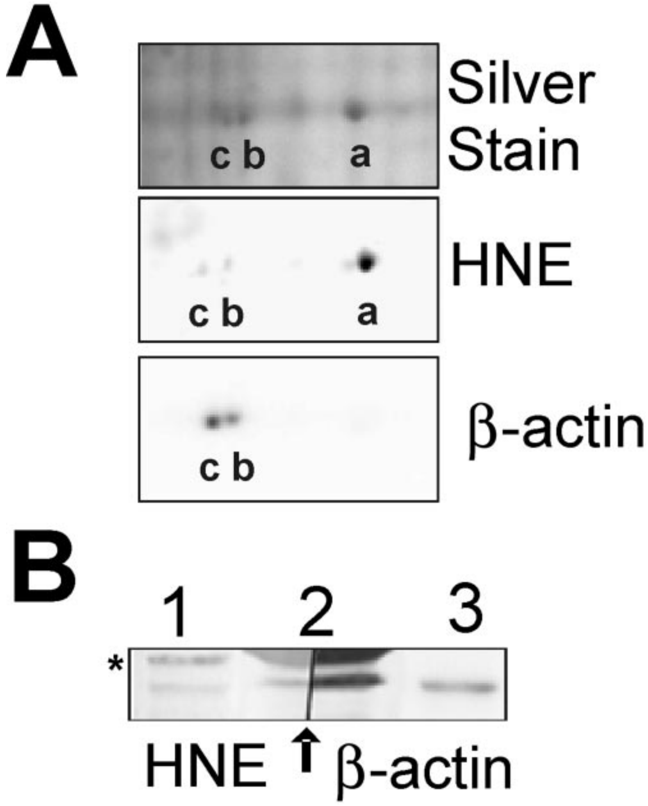

FIGURE 3. Validation of HNE-modified proteins. (**A**) Section of silver-stained 2-D gel (*top*) and 2-D Western blot (probed with HNE and β-actin antibodies) corresponding to spots 14a, -b, and -c (Fig. 1). (**B**) Immunoprecipitation of β-actin. *Lane 1*: retinal homogenate; *lane 2*: immunoprecipitated β-actin; *lane 3*: retinal homogenate. *Arrow*: split of *lane 2*. The area to the *left* of the *arrow* was probed with anti-HNE. The area to the *right* of the *arrow* was probed with anti-β-actin. The lower band shows reactivity of β-actin in all *lanes*. *Asterisk* represents another HNE-immune reactive protein in *lane 1* and reactivity of the IgG heavy chains in *lane 2*.

CK is HNE-modified. To investigate whether β-actin was also modified, we immunoprecipitated β-actin from retinal homogenates and then probed for HNE adducts (Fig. 3B). Our results show a positive immune reaction for HNE in the precipitated β-actin protein band. We conclude that both CK and β-actin contain HNE adducts, which is consistent with previous reports of HNE modification and carbonyl modification, respectively.[43,44]

With all other immune positive spots, only a single protein matched the peptide mass fingerprint. As an additional control to check for multiple proteins, we re-examined the data from full-scan MALDI by first removing the peptides that matched the identified protein and then searched for matches to additional proteins. This secondary analysis resulted in no additional proteins detected in any immune-reactive spot.

Quantification of Total HNE

While 2-D Western blot analysis allowed us to evaluate the distribution of HNE-reactive protein spots, it is not an optimal method for quantifying the relative HNE content because of the intrinsic limitations of 2D gels. First, membrane proteins are poorly resolved. The position of membrane proteins at the site of HNE formation suggests these proteins may contain a significant number of HNE-adducts that would be missed by 2D analysis. A second limitation includes the difficulty in detecting HNE-modified proteins that are present in low abundance. To overcome these limitations, we used a slot blot immunoassay to assess the total relative content of HNE-modified proteins.

Proteins from both the macula and periphery were analyzed for total HNE-protein content. As seen in Figure 4, no change in relative HNE content was observed between the stages of AMD in either the macula ($P = 0.16$) or the periphery ($P = 0.93$). In addition, no change was detected when control tissue (MGS1) was compared to diseased tissue (MGS2 to 4) in the macula ($P = 0.40$) or periphery ($P = 0.86$). When all stages per region were combined, no significant change ($P = 0.51$) in relative content was observed between the macula (7.6 ± 0.7 AUF/mg) and the periphery (6.6 ± 0.7 AUF/mg).

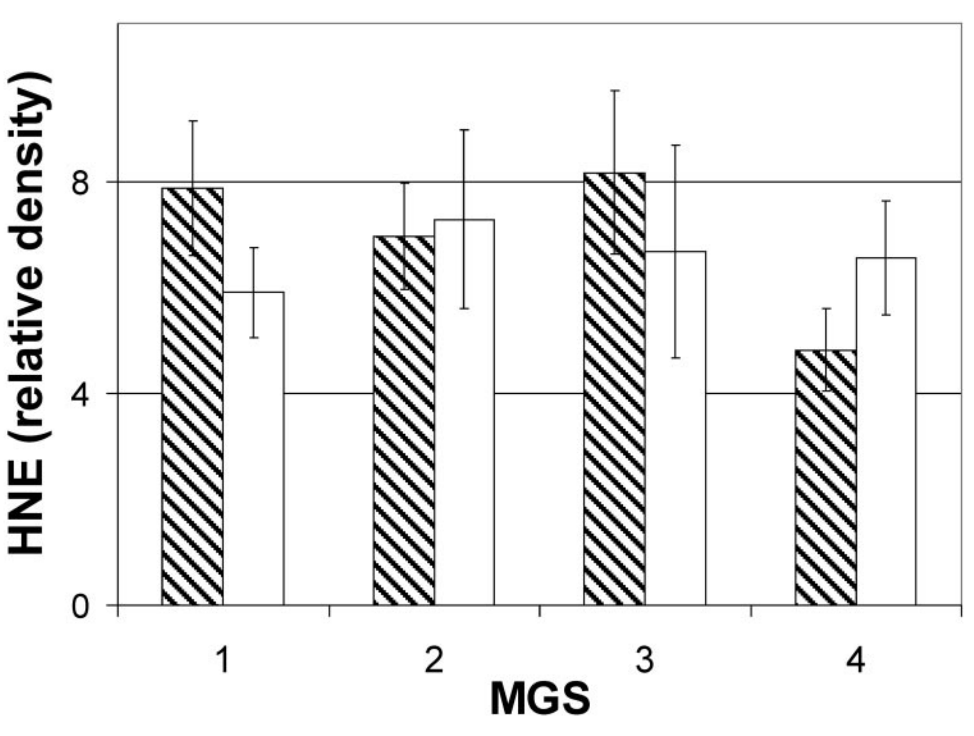

FIGURE 4. Quantification of the relative content of HNE-modified proteins. Data are the density (mean ± SEM) of the immune reaction on slot blots. MGS1 to -4 levels are shown in both the macular (*hatched*) and peripheral (*solid*) regions. All reactions were normalized to the reaction of HNE-modified BSA run on each blot. The relative content in each sample was determined from two to four separate replicates. $n = 6$ in each group of donors.

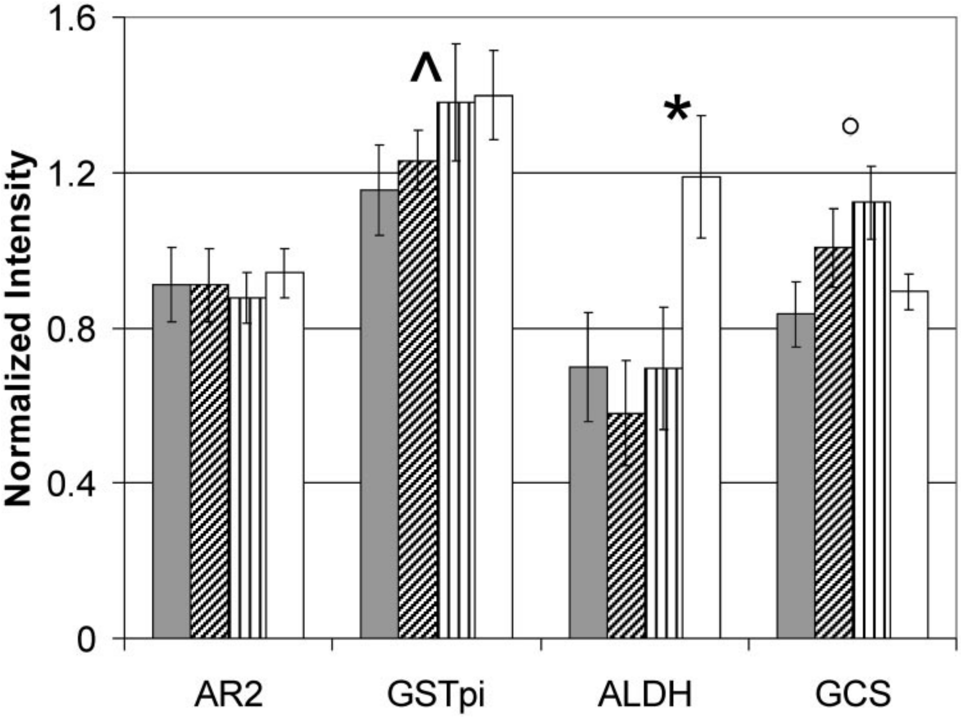

Figure 5. Semiquantitative analysis of proteins involved in HNE detoxification. Data are the mean (±SEM) densities of immune reactions by 1-D Western blot for MGS 1 (*gray*), MGS2 (*hatched*), MGS3 (*vertical*), MGS4 (*white*) bars. $^{\wedge}P \leq 0.1$ all stages; $^{*}P \leq 0.05$ all stages; $^{\circ}P \leq 0.05$ MGS1 to three by linear regression. $N = 9$ to 11 for each stage (peripheral retina).

Pathways for HNE Detoxification

Because our measurements have shown no difference in either the extent or pattern of HNE-modified proteins, one possibility is that the cellular detoxification systems directed at HNE are adequate regardless of the disease stage. Previous studies have shown that the detoxifying enzymes are upregulated when the cells are exposed to oxidative stress.[35–38] Therefore, the cellular content of these enzymes provide an indication of the cells' response to oxidative stress. We evaluated the content of several proteins involved in detoxifying or removing HNE from the cell as an indirect indicator of cellular levels of HNE. We measured the content of three enzymes that directly detoxify HNE in the cell: aldehyde dehydrogenase (ALDH), aldose reductase (AR), and glutathione-*S*-transferase (GST). These enzymes detoxify HNE via oxidation to 4-hydroxy-2-nonenoic acid (HNA),[45] reduction to 1,4-dihydroxy-2-nonene (DHN),[46] or conjugation with glutathione (GSH).[47] Two of the three proteins directly involved in detoxification show a modest increase in expression. Our results show ALDH was significantly increased in content ($P = 0.02$) and GSTpi showed a trend toward a significant increase ($P = 0.07$), although AR exhibited no change in content ($P = 0.85$; Fig. 5). In addition, glutamyl cysteine synthetase (GCS), the rate-limiting enzyme in the formation of GSH, showed no significant change ($P = 0.53$) in content when considering all four MGS stages. However, a linear increase ($P = 0.04$) of GCS content was observed through MGS3.

Discussion

This study tested the hypothesis that an increase in oxidative damage to the retina is associated with the pathogenesis and progression of AMD. Specifically, we predicted that the highly toxic oxidation product, HNE, would accumulate during disease progression. HNE is produced from the peroxidation of ω-6-polyunsaturated fatty acids of membrane lipids (Fig. 6). Multiple pathways for detoxifying HNE to a less toxic compound help prevent cellular damage. However, if these pathways are inadequate, HNE can form adducts with DNA, lipid, and proteins both within and outside the membrane where it is produced.[22] The concentration of HNE-modified proteins reflects the balance between HNE-protein adduct formation

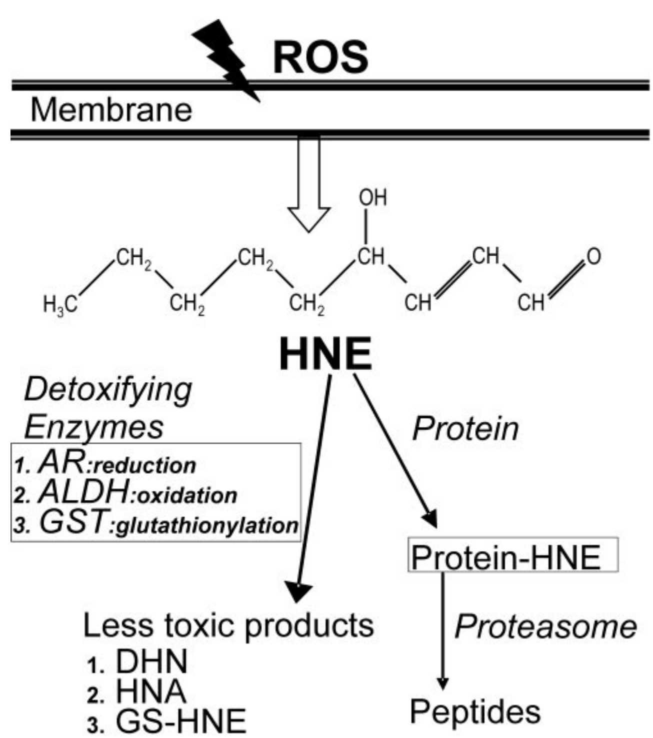

Figure 6. HNE formation and pathways of elimination. Oxidation of membranes by reactive oxygen species (ROS) generates HNE. If HNE is not directly detoxified through enzymatic reactions with aldose reductase (AR), aldehyde dehydrogenase (ALDH), or glutathione-*S*-transferase (GST), it can modify proteins. HNE-proteins are eliminated by proteasome degradation.[49]

resulting from peroxidation of membrane lipids and the elimination of HNE by detoxifying enzymes[48] or the removal of modified proteins by the proteasome.[49] In the present study, we examined the content of both protein HNE adducts and several enzymes involved in the detoxification pathway, to determine whether elevated HNE adducts correlate with AMD. Because the level of HNE-protein adducts was not significantly altered between MGS stages, either the cellular production of HNE remains constant or the enzymes involved in elimination of HNE or HNE-modified proteins are upregulated.

As a caveat regarding our finding that HNE-adducted proteins do not accumulate with AMD, the high variability of donor tissue could prevent distinguishing stage-specific differences in HNE-modified proteins. In addition to donor genetics and environmental conditions that contribute to the variability, there is also the overlap of phenotypes and subsequent imprecise categorization of donors using the current grading system, which is especially relevant for MGS3. Future studies may require the use of more highly defined stages as reported recently in a nine-point grading scale.[50] An additional caveat is that the constraints of proteomic technology may have limited our ability to find statistically significant differences. For example, modified proteins present in low abundance, poorly resolved membrane proteins, or proteins outside the pH range of 5 to 8 would be beyond the level of detection. Slot blot assays were used to overcome some of these limitations. However, modification of functionally important proteins in low abundance would be below the detection threshold for all assays used in the present study.

The content of several proteins involved in detoxifying HNE were measured to test whether these proteins are upregulated with AMD. Although GSTpi has comparatively lower activity for HNE (~0.5–1.5 micromoles/[mg · min])[51] than other GST family members, such as GSTA4-4 or hGST5.8 (~180–190 micromoles/[mg · min]),[51–53] it may still contribute substantially to detoxification due to its high abundance in human retinal tissues. We attempted to measure GSTA4-4, but it was undetected in up to 150 μg of protein (data not shown). This is probably due to low cellular content and/or poor reactivity of the antibody in human tissue.[54–56]

Of the four proteins examined, the content of three (GSTpi, ALDH, and GCS) was modestly upregulated with AMD. These proteins have been shown to increase after oxidative stress,[35–38] indicating that they respond to changes in cellular redox status. Although these proteins or their products are involved in detoxifying HNE, they can also detoxify other molecules or perform other functions in the cell.[45,57,58] Therefore, the increased cellular content of proteins involved in detoxifying HNE may be a compensatory response to elevated cellular levels of HNE and/or other by-products of oxidative stress or may reflect changes in alternative functions of these proteins. However, the extent of protection provided by the small increase in content is currently unclear.

The large number of proteins containing HNE adducts confirms that HNE is a major oxidant in the retina. Corroborating studies show a significant amount of HNE-modified proteins with light-induced damage[27,59] and increasing age[28,60] and in a pig model of retinitis pigmentosa.[29] HNE-modified proteins in the photoreceptors exert their toxic effects on the retinal pigment epithelium (RPE) via the induction of angiogenic cytokines[61] or accelerated lipofuscinogenesis.[62] Lipofuscin is composed of undigested components of photoreceptor outer segments (POS) that were phagocytosed.[13,14,62–64] Proteomic analyses of lipofuscin from RPE of human donor eyes confirmed the presence of both MDA and HNE adducts on POS protein.[13,14,65] The toxic effect of lipofuscin results from generation of free radicals in the presence of blue light.[66] This mechanism is proposed to be involved in cellular apoptosis associated with AMD.[66] Although it is unclear whether lipofuscin accumulates with AMD, it is possible that continuous consumption of HNE-modified proteins becomes cytotoxic at later stages when the damaged RPE are less able to accommodate the phagocytic load.

An important consideration is whether HNE-adducts induce changes in protein function. It is possible that most of the modifications are functionally silent. Alternatively, HNE modification at a critical site (i.e., in or near the active site or at structurally sensitive sites), could impair protein function. HNE-induced inhibition of protein function has been shown for many proteins[24,67,68] including both CK[69] and pyruvate dehydrogenase,[70] identified in the present study. The functional effect of inhibiting a subpopulation of proteins could be amplified if multiple proteins in a pathway are involved. In one example from our data, several modified proteins in the glycolytic pathway (TPI, enolase, aldolase) contained HNE-adducts. Because a major source of energy for the retina is derived directly from the glycolytic pathway,[71] the dysfunction of glycolytic proteins may have a significant impact on retinal cell function.

The consistent HNE modification of specific proteins, regardless of the donor stage or region, suggests that these proteins are preferentially modified by HNE. The proteins identified in this study share substantial overlap with oxidatively modified proteins observed in other models, tissues, or species,[14,28,43,44,72–75] suggesting the existence of preferred molecular targets of reactive aldehyde and oxygen species. HNE may target specific proteins due to their abundance, proximity to membranes, or the presence of surface reactive amino acids. One would predict that abundant proteins provide the greatest number of targets. However, not all the identified HNE-modified proteins in this study are highly abundant (ex. #1, Fig. 1). The proximity of proteins near membranes would also increase their susceptibility to modifications. For example, glyceraldehyde-3-phosphate dehydrogenase (GAPDH), TPI (#4), and aldolase (#3) form a complex[76,77] that electrostatically interacts with the mitochondrial membrane.[78] (HNE modification of GAPDH was observed by 1-D immunoblot methods; data not shown). Finally, several proteins identified in this study—TPI (#4), aldolase (#3), and α-enolase (#2)—are reversibly glutathionylated on reactive cysteine residues to regulate enzymatic activity.[28,79] These reactive cysteine sulfhydryls are readily modified by HNE and thus may increase a protein's susceptibility to HNE modification.

In summary, our data show that a large number of retinal proteins contain HNE adducts, suggesting that HNE is a major oxidant in the retina. These proteins are consistently modified and represent preferred targets for the cytotoxic oxidant, HNE. Our list of proteins can serve as a basis for future studies to test the functional effect of HNE modification on these specific proteins.

HNE-modified proteins do not accumulate in the neurosensory retina during progression of AMD, implying that pathways involved in detoxification of HNE or removal of HNE-modified proteins are adequate to prevent accumulation. In the field of AMD biology, a current point of interest has been in establishing reliable biomarkers to monitor disease progression or measure the relative success of specific treatments. HNE has been suggested (but not experimentally tested) as a potential biomarker for AMD. Although other models of retinal degeneration (i.e., light-induced damage) have shown increased HNE content, our results suggest that HNE is not a sensitive retinal biomarker for AMD. Based on the strength of our experimental design (the use of a reasonable sample size of human donor tissue, separate analyses of macula and periphery, comparison of control versus three progressive stages of AMD using multiple analytical methods), we feel confident that our answer is not misguided and provides important physiologically and clinically relevant information. Although we have investigated only one of many different oxidation products, other products of oxidative damage, such as nitration, advanced glycation end-products, or carboxyethylpyrrole may accumulate with the disease and serve as more sensitive retinal biomarkers for AMD. However, since our measures were confined to the retina, which we feel is most relevant for understanding disease mechanisms, it does not exclude the possibility that serum levels of HNE and other products of oxidation would be elevated if systemic oxidative stress plays a key role in AMD.

Acknowledgments

The authors thank the Minnesota Lions Eye Bank for their assistance in procuring eyes for the study; Curt Nordgaard and Pabalu Karunadharma for careful review of the manuscript; Kristin Berg and Kristin Pilon for assistance with the retinal dissections; and the Mass Spectrometry Consortium for the Life Sciences at the University of Minnesota for technical assistance.

References

1. Klein BE, Klein R. Cataracts and macular degeneration in older Americans. *Arch Ophthalmol*. 1982;100:571–573.
2. Klein R, Klein BE, Linton KL. Prevalence of age-related maculopathy. The Beaver Dam Eye Study. *Ophthalmology*. 1992;99:933–943.
3. Klaver CC, Wolfs RC, Vingerling JR, Hofman A, de Jong PT. Age-specific prevalence and causes of blindness and visual impairment in an older population: the Rotterdam Study. *Arch Ophthalmol*. 1998;116:653–658.
4. The Age-Related Eye Disease Study system for classifying age-related macular degeneration from stereoscopic color fundus photographs: the Age-Related Eye Disease Study Report Number 6. *Am J Ophthalmol.* 2001;132:668–681.
5. Olsen TW, Feng X. The Minnesota Grading System of eyebank eyes for age-related macular degeneration. *Invest Ophthalmol Vis Sci.* 2004;45:4484–4490.
6. Ethen CM, Reilly C, Feng X, Olsen TW, Ferrington DA. The proteome of central and peripheral retina with progression of age-related macular degeneration. *Invest Ophthalmol Vis Sci*. 2006;47:2280–2290.
7. Nordgaard CL, Berg KM, Kapphahn RJ, et al. Proteomics of the retinal pigment epithelium reveals altered protein expression at progressive stages of age-related macular degeneration. *Invest Ophthalmol Vis Sci*. 2006;47:815–822.
8. Ethen CM, Feng X, Olsen TW, Ferrington DA. Declines in arrestin and rhodopsin in the macula with progression of age-related macular degeneration. *Invest Ophthalmol Vis Sci*. 2005;46:769–775.
9. Vingerling JR, Hofman A, Grobbee DE, de Jong PT. Age-related macular degeneration and smoking. The Rotterdam Study. *Arch Ophthalmol*. 1996;114:1193–1196.
10. Cruickshanks KJ, Klein R, Klein BE. Sunlight and age-related macular degeneration. The Beaver Dam Eye Study. *Arch Ophthalmol*. 1993;111:514–518.
11. A randomized, placebo-controlled, clinical trial of high-dose supplementation with vitamins C and E, beta carotene, and zinc for age-related macular degeneration and vision loss: AREDS report no. 8. *Arch Ophthalmol.* 2001;119:1417–1436.
12. Hahn P, Milam AH, Dunaief JL. Maculas affected by age-related macular degeneration contain increased chelatable iron in the retinal pigment epithelium and Bruch's membrane. *Arch Ophthalmol*. 2003;121:1099–1105.
13. Warburton S, Southwick K, Hardman RM, et al. Examining the proteins of functional retinal lipofuscin using proteomic analysis as a guide for understanding its origin. *Mol Vis*. 2005;11:1122–1134.
14. Schutt F, Bergmann M, Holz FG, Kopitz J. Proteins modified by malondialdehyde, 4-hydroxynonenal, or advanced glycation end products in lipofuscin of human retinal pigment epithelium. *Invest Ophthalmol Vis Sci*. 2003;44:3663–3668.
15. Crabb JW, Miyagi M, Gu X, et al. Drusen proteome analysis: an approach to the etiology of age-related macular degeneration. *Proc Natl Acad Sci USA*. 2002;99:14682–14687.
16. Imamura Y, Noda S, Hashizume K, et al. Drusen, choroidal neovascularization, and retinal pigment epithelium dysfunction in SOD1-deficient mice: a model of age-related macular degeneration. *Proc Natl Acad Sci USA*. 2006;103:11282–11287.
17. Beatty S, Koh H, Phil M, Henson D, Boulton M. The role of oxidative stress in the pathogenesis of age-related macular degeneration. *Surv Ophthalmol*. 2000;45:115–134.
18. Totan Y, Cekic O, Borazan M, Uz E, Sogut S, Akyol O. Plasma malondialdehyde and nitric oxide levels in age related macular degeneration. *Br J Ophthalmol*. 2001;85:1426–1428.
19. Gu X, Meer SG, Miyagi M, et al. Carboxyethylpyrrole protein adducts and autoantibodies, biomarkers for age-related macular degeneration. *J Biol Chem*. 2003;278:42027–42035.
20. Ishibashi T, Murata T, Hangai M, et al. Advanced glycation end products in age-related macular degeneration. *Arch Ophthalmol*. 1998;116:1629–1632.
21. Hammes HP, Hoerauf H, Alt A, et al. N(epsilon)(carboxymethyl)lysin and the AGE receptor RAGE colocalize in age-related macular degeneration. *Invest Ophthalmol Vis Sci*. 1999;40:1855–1859.
22. Esterbauer H, Schaur RJ, Zollner H. Chemistry and biochemistry of 4-hydroxynonenal, malonaldehyde and related aldehydes. *Free Radic Biol Med*. 1991;11:81–128.
23. Negre-Salvayre A, Vieira O, Escargueil-Blanc I, Salvayre R. Oxidized LDL and 4-hydroxynonenal modulate tyrosine kinase receptor activity. *Mol Aspects Med*. 2003;24:251–261.
24. Ferrington DA, Kapphahn RJ. Catalytic site-specific inhibition of the 20S proteasome by 4-hydroxynonenal. *FEBS Lett*. 2004;578:217–223.
25. Crabb JW, O'Neil J, Miyagi M, West K, Hoff HF. Hydroxynonenal inactivates cathepsin B by forming Michael adducts with active site residues. *Protein Sci*. 2002;11:831–840.
26. Szweda LI, Uchida K, Tsai L, Stadtman ER. Inactivation of glucose-6-phosphate dehydrogenase by 4-hydroxy-2-nonenal. Selective modification of an active-site lysine. *J Biol Chem*. 1993;268:3342–3347.
27. Tanito M, Elliott MH, Kotake Y, Anderson RE. Protein modifications by 4-hydroxynonenal and 4-hydroxyhexenal in light-exposed rat retina. *Invest Ophthalmol Vis Sci*. 2005;46:3859–3868.
28. Kapphahn RJ, Giwa BM, Berg KM, et al. Retinal proteins modified by 4-hydroxynonenal: identification of molecular targets. *Exp Eye Res*. 2006;83:165–175.
29. Shen J, Yang X, Dong A, et al. Oxidative damage is a potential cause of cone cell death in retinitis pigmentosa. *J Cell Physiol*. 2005;203:457–464.
30. De La Paz MA, Anderson RE. Lipid peroxidation in rod outer segments. Role of hydroxyl radical and lipid hydroperoxides. *Invest Ophthalmol Vis Sci*. 1992;33:2091–2096.
31. De La Paz MA, Zhang J, Fridovich I. Antioxidant enzymes of the human retina: effect of age on enzyme activity of macula and periphery. *Curr Eye Res*. 1996;15:273–278.
32. van Kuijk FJ, Buck P. Fatty acid composition of the human macula and peripheral retina. *Invest Ophthalmol Vis Sci*. 1992;33:3493–3496.
33. Laemmli UK. Cleavage of structural proteins during the assembly of the head of bacteriophage T4. *Nature*. 1970;227:680–685.
34. Friedman DS, Katz J, Bressler NM, Rahmani B, Tielsch JM. Racial differences in the prevalence of age-related macular degeneration: the Baltimore Eye Survey. *Ophthalmology*. 1999;106:1049–1055.
35. Ho Koh Y, Seek Park Y, Takahashi M, Suzuki K, Taniguchi N. Aldehyde reductase gene expression by lipid peroxidation end products, MDA and HNE. *Free Radic Res*. 2001;33:739–746.
36. Keightley JA, Shang L, Kinter M. Proteomic analysis of oxidative stress-resistant cells: a specific role for aldose reductase overexpression in cytoprotection. *Mol Cell Proteomics*. 2004;3:167–175.
37. Hayes JD, Flanagan JU, Jowsey IR. Glutathione transferases. *Annu Rev Pharmacol Toxicol*. 2005;45:51–88.
38. Cheng JZ, Sharma R, Yang Y, et al. Accelerated metabolism and exclusion of 4-hydroxynonenal through induction of RLIP76 and hGST5.8 is an early adaptive response of cells to heat and oxidative stress. *J Biol Chem*. 2001;276:41213–41223.

39. Uchida K, Szweda LI, Chae HZ, Stadtman ER. Immunochemical detection of 4-hydroxynonenal protein adducts in oxidized hepatocytes. *Proc Natl Acad Sci USA*. 1993;90:8742–8746.
40. Colvis C, Garland D. Posttranslational modification of human alphaA-crystallin: correlation with electrophoretic migration. *Arch Biochem Biophys*. 2002;397:319–323.
41. Dunbar BS. Basic principles of post-translational modifications of proteins and their analysis using high resolution two-dimensional polyacrylamide gel electrophoresis. *Two-dimensional Electrophoresis and Immunological Techniques.* New York: Plenum; 1988;77–98.
42. Ueda Y, Duncan MK, David LL. Lens proteomics: the accumulation of crystallin modifications in the mouse lens with age. *Invest Ophthalmol Vis Sci*. 2002;43:205–215.
43. Hussain SN, Matar G, Barreiro E, Florian M, Divangahi M, Vassilakopoulos T. Modifications of proteins by 4-hydroxy-2-nonenal in the ventilatory muscles of rats. *Am J Physiol*. 2006;290:L996–L1003.
44. Butterfield DA. Amyloid beta-peptide (1–42)-induced oxidative stress and neurotoxicity: implications for neurodegeneration in Alzheimer's disease brain: a review. *Free Radic Res*. 2002;36:1307–1313.
45. Vasiliou V, Pappa A, Petersen DR. Role of aldehyde dehydrogenases in endogenous and xenobiotic metabolism. *Chem Biol Interact*. 2000;129:1–19.
46. Srivastava S, Chandra A, Bhatnagar A, Srivastava SK, Ansari NH. Lipid peroxidation product, 4-hydroxynonenal and its conjugate with GSH are excellent substrates of bovine lens aldose reductase. *Biochem Biophys Res Commun*. 1995;217:741–746.
47. Alin P, Danielson UH, Mannervik B. 4-Hydroxyalk-2-enals are substrates for glutathione transferase. *FEBS Lett*. 1985;179:267–270.
48. Choudhary S, Srivastava S, Xiao T, Andley UP, Srivastava SK, Ansari NH. Metabolism of lipid derived aldehyde, 4-hydroxynonenal in human lens epithelial cells and rat lens. *Invest Ophthalmol Vis Sci*. 2003;44:2675–2682.
49. Grune T, Davies KJ. The proteasomal system and HNE-modified proteins. *Mol Aspects Med*. 2003;24:195–204.
50. Davis MD, Gangnon RE, Lee LY, et al. The Age-Related Eye Disease Study severity scale for age-related macular degeneration: AREDS Report No. 17. *Arch Ophthalmol*. 2005;123:1484–1498.
51. Singhal SS, Zimniak P, Awasthi S, et al. Several closely related glutathione S-transferase isozymes catalyzing conjugation of 4-hydroxynonenal are differentially expressed in human tissues. *Arch Biochem Biophys*. 1994;311:242–250.
52. Hubatsch I, Ridderstrom M, Mannervik B. Human glutathione transferase A4–4: an alpha class enzyme with high catalytic efficiency in the conjugation of 4-hydroxynonenal and other genotoxic products of lipid peroxidation. *Biochem J*. 1998;330:175–179.
53. Singhal SS, Zimniak P, Sharma R, Srivastava SK, Awasthi S, Awasthi YC. A novel glutathione S-transferase isozyme similar to GST 8–8 of rat and mGSTA4–4 (GST 5.7) of mouse is selectively expressed in human tissues. *Biochim Biophys Acta*. 1994;1204:279–286.
54. Desmots F, Rissel M, Loyer P, Turlin B, Guillouzo A. Immunohistological analysis of glutathione transferase A4 distribution in several human tissues using a specific polyclonal antibody. *J Histochem Cytochem*. 2001;49:1573–1580.
55. Coles BF, Kadlubar FF. Human alpha class glutathione S-transferases: genetic polymorphism, expression, and susceptibility to disease. *Methods Enzymol*. 2005;401:9–42.
56. McGuire S, Daggett D, Bostad E, Schroeder S, Siegel F, Kornguth S. Cellular localization of glutathione S-transferases in retinas of control and lead-treated rats. *Invest Ophthalmol Vis Sci*. 1996;37:833–842.
57. Petrash JM. All in the family: aldose reductase and closely related aldo-keto reductases. *Cell Mol Life Sci*. 2004;61:737–749.
58. Kathmann EC, Naylor S, Lipsky JJ. Rat liver constitutive and phenobarbital-inducible cytosolic aldehyde dehydrogenases are highly homologous proteins that function as distinct isozymes. *Biochemistry*. 2000;39:11170–11176.
59. Rex TS, Tsui I, Hahn P, et al. Adenovirus-mediated delivery of catalase to retinal pigment epithelial cells protects neighboring photoreceptors from photo-oxidative stress. *Hum Gene Ther*. 2004;15:960–967.
60. Louie JL, Kapphahn RJ, Ferrington DA. Proteasome function and protein oxidation in the aged retina. *Exp Eye Res*. 2002;75:271–284.
61. Higgins GT, Wang JH, Dockery P, Cleary PE, Redmond HP. Induction of angiogenic cytokine expression in cultured RPE by ingestion of oxidized photoreceptor outer segments. *Invest Ophthalmol Vis Sci*. 2003;44:1775–1782.
62. Wihlmark U, Wrigstad A, Roberg K, Brunk UT, Nilsson SE. Formation of lipofuscin in cultured retinal pigment epithelial cells exposed to pre-oxidized photoreceptor outer segments. *APMIS*. 1996;104:272–279.
63. Kopitz J, Holz FG, Kaemmerer E, Schutt F. Lipids and lipid peroxidation products in the pathogenesis of age-related macular degeneration. *Biochimie* (*Paris*). 2004;86:825–831.
64. Winkler BS, Boulton ME, Gottsch JD, Sternberg P. Oxidative damage and age-related macular degeneration. *Mol Vis*. 1999;5:32.
65. Schutt F, Ueberle B, Schnolzer M, Holz FG, Kopitz J. Proteome analysis of lipofuscin in human retinal pigment epithelial cells. *FEBS Lett*. 2002;528:217–221.
66. Sparrow JR, Zhou J, Ben-Shabat S, Vollmer H, Itagaki Y, Nakanishi K. Involvement of oxidative mechanisms in blue-light-induced damage to A2E-laden RPE. *Invest Ophthalmol Vis Sci*. 2002;43:1222–1227.
67. Ishii T, Tatsuda E, Kumazawa S, Nakayama T, Uchida K. Molecular basis of enzyme inactivation by an endogenous electrophile 4-hydroxy-2-nonenal: identification of modification sites in glyceraldehyde-3-phosphate dehydrogenase. *Biochemistry*. 2003;42:3474–3480.
68. Del Corso A, Dal Monte M, Vilardo PG, et al. Site-specific inactivation of aldose reductase by 4-hydroxynonenal. *Arch Biochem Biophys*. 1998;350:245–248.
69. Horakova E, Ondrejickova O, Vajdova M, Korytar P, Durackova Z, Schaur RJ. Mechanisms of iron-induced oxidative modifications of creatine kinase in rat brain in vitro: possible involvement of HNE. *Gen Physiol Biophys*. 2002;21:327–336.
70. Humphries KM, Szweda LI. Selective inactivation of alpha-ketoglutarate dehydrogenase and pyruvate dehydrogenase: reaction of lipoic acid with 4-hydroxy-2-nonenal. *Biochemistry*. 1998;37:15835–15841.
71. Winkler BS. A quantitative assessment of glucose metabolism in the isolated rat retina. In: Christen Y, Doly M, Droy-Lefaix M, eds. *Les Seminaires Ophtalmologiques d'IPSEN.* Paris: Elsevier; 1995;78–96.
72. Miyagi M, Sakaguchi H, Darrow RM, et al. Evidence that light modulates protein nitration in rat retina. *Mol Cell Proteomics*. 2002;1:293–303.
73. Tezel G, Yang X, Cai J. Proteomic identification of oxidatively modified retinal proteins in a chronic pressure-induced rat model of glaucoma. *Invest Ophthalmol Vis Sci*. 2005;46:3177–3187.
74. Stagsted J, Bendixen E, Andersen HJ. Identification of specific oxidatively modified proteins in chicken muscles using a combined immunologic and proteomic approach. *J Agric Food Chem*. 2004;52:3967–3974.
75. Perluigi M, Fai Poon H, Hensley K, et al. Proteomic analysis of 4-hydroxy-2-nonenal-modified proteins in G93A-SOD1 transgenic mice–a model of familial amyotrophic lateral sclerosis. *Free Radic Biol Med*. 2005;38:960–968.
76. Stephan P, Clarke F, Morton D. The indirect binding of triose-phosphate isomerase to myofibrils to form a glycolytic enzyme mini-complex. *Biochim Biophys Acta*. 1986;873:127–135.
77. Beeckmans S, Van Driessche E, Kanarek L. Clustering of sequential enzymes in the glycolytic pathway and the citric acid cycle. *J Cell Biochem*. 1990;43:297–306.
78. Hartmann CM, Gehring H, Christen P. The mature form of imported mitochondrial proteins undergoes conformational changes upon binding to isolated mitochondria. *Eur J Biochem*. 1993;218:905–910.
79. Fratelli M, Demol H, Puype M, et al. Identification of proteins undergoing glutathionylation in oxidatively stressed hepatocytes and hepatoma cells. *Proteomics*. 2003;3:1154–1161.